Computers and Concrete, Vol. 4, No. 5 (2007) 331-346
DOI: http://dx.doi.org/10.12989/cac.2007.4.5.331

Performance analysis tool for reinforced concrete members

Asad Esmaeily† and Robert J. Peterman‡

Civil Engineering Department, Kansas State University, Manhattan, KS 66506, USA

(Received January 21, 2006, Accepted October 6, 2006)

Abstract. A computer program was developed to analyze the non-linear, cyclic flexural performance of reinforced concrete structural members under various types of loading paths including non-sequential variations in axial load. This performance is significantly affected by the loading history. Different monotonic material models as well as hysteresis rules for confined and unconfined concrete and steel, some developed and calibrated against test results on material samples, were implemented in a fiber-based moment-curvature and in turn force-deflection analysis. One of the assumptions on curvature distribution along the member was based on a method developed to address the variation of the plastic hinge length as a result of loading pattern. Functionality of the program was verified by reproduction of analytical results obtained by others for several cases, and accuracy of the analytical process and the implemented models were evaluated against the experimental results from large-scale reinforced concrete columns tested under the analyzed loading cases. While the program can be used to predict the response of a member under a certain loading pattern, it can also be used to examine various analytical models and methods or refine a custom material model against test data.

Keywords: analysis; force-deflection; load pattern; material model; moment-curvature; performance; variable axial load.

1. Introduction

Structural design methodologies have evolved over the years. Initially, “Allowable Stress Design” was the approach followed by most designers. Currently, “Load and Resistance Factor Design” (LRFD) is most often used by engineers. Both of these design methods focus on individual structural elements and ensure that none will experience loads or deformations greater than their design capacity. Performance-Based Design (PBD) as a new emerging design methodology seeks to ensure that a structure will perform in some predictable way. Performance of a structure during its lifetime and specifically its behavior under various loading conditions provides the foundation for PBD. Depending on the expected functionality of a structure, specific objectives are set for its performance during its service life-time. These objectives may be the allowable level of damage for the structure as a whole under a certain loading condition during its life-time; or conditions for a member; such as cracking, yielding, deformations, etc., when subjected to specific service loads.

† Assistant Professor, E-mail: asad@k-state.edu
‡ Associate Professor, E-mail: bob@k-state.edu

Employment of analytical methods capable of providing realistic predictions of the behavior and ultimate strength and deformability of structural systems is one of the main analytical components of performance-based design. Estimation of the inflicted damage on a structural element or occurrence of a certain limit state with a reasonable accuracy requires a realistic prediction of the performance of a structure. Accuracy of the analytical predictions and assessments depends on the employed analytical methods and implemented material models, constitutive laws and Hysteresis rules. Sophisticated methods such as a detailed finite element analysis along with advanced material models and proper constitutive laws are an option; however, this is not the first choice for a design engineer who prefers less sophisticated approaches along with simplified material models to achieve a targeted accuracy.

The available computer applications are mostly limited to section analysis under a constant axial load and monotonic, and very few cyclic, lateral displacement or force. The computer program described in this paper, implements relatively simple analytical methods and material models to predict the performance of reinforced concrete structures under various loading conditions, including cyclic lateral displacement under a non-proportionally variable axial load, with an acceptable accuracy. This prediction is necessary for the flexural capacity and performance assessment of reinforced concrete columns subjected to the combined effect of uncoupled variations of lateral and axial load.

This application is also a useful analytical tool to examine the accuracy of various material models, hysteresis rules, and other assumptions, in simulating the response of a reinforced concrete member tested under a certain loading pattern. In an earlier work by the author (Esmaeily and Lucio 2006), the accuracy of some representative models for monotonic response of confined concrete was studied using this application as the main analysis tool.

2. Development of the computer-based analytical tool

The basic goal was developing a simple analytical tool to predict the non-linear performance of reinforced concrete members, especially bridge or building columns, under various loading paths with enough options and flexibility in terms of the material models and analytical assumptions. The loading patterns include any combination or axial load variation and lateral force or displacement pattern. The program is a Windows-based application with a friendly interface and various options in terms of the input data, analytical methods and models, and the output data.

Analysis is based on fiber modeling of the section and in turn the member, as the backbone analytical method, effectively used by others (Mazzoni, *et al.* 2006, CSI Section Builder 2003, Parakash, *et al.* 1993). By providing the hysteresis stress-strain behavior of the confined and unconfined concrete and steel, this model can be used to analyze the behavior of a reinforced concrete section under any loading pattern.

The geometry; reinforcement arrangement, size and amount, can effectively be assigned through the interface. All other factors such as material models, hysteresis rules, assumption on curvature distribution on the member including different plastic hinge models, accuracy of the analysis in terms of fineness of the mesh and number of data points, and the type of analysis can be selected or set by the user.

A displacement-controlled analysis, as an option, makes it possible to capture the post-peak performance of the member. Force-deflection analysis is based on the section analysis at several

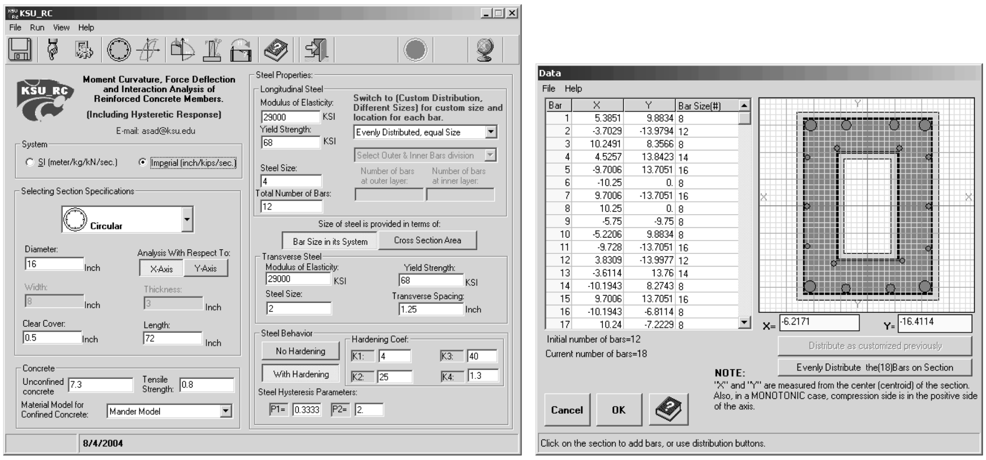

Fig. 1 The main window and the interactive window for a customized section

locations required by the assumption on curvature distribution along the member, including the new method developed to address the variation of the plastic-hinge length under a variable axial load and cyclic lateral displacement.

The effect of confinement is considered in the monotonic stress-strain relationship models of concrete confined by the lateral reinforcement. The monotonic curve serves as the envelope for the hysteresis response for the models. Strain hardening of the steel can be considered in the analysis.

Fig. 1 shows the main window and an instance of a sample customized cross section of the application. The application, KSU_RC, under revision to implement more options and models, can be freely downloaded at: http://www.ce.ksu.edu/faculty/esmaeily (Esmaeily 2004).

This application is being used for educational purposes at some schools and is regarded as a simple free performance assessment tool by some design firms. A brief description of the analysis process and the material models and methods developed and implemented in the program is as follows.

2.1. Summary of the analysis process

For a moment-curvature analysis, the section is defined in terms of its geometry and reinforcement type and arrangement in the longitudinal and transverse directions; material properties are set for steel and concrete in terms of their monotonic and cyclic responses; and moment-curvature analysis, as discussed later, is performed based on the selected loading condition and type of the analysis.

For a monotonic or cyclic curvature in a “displacement-controlled analysis” or a monotonic or cyclic moment in a “force-controlled analysis”, the axial load can be constant or variable. The variation in axial load can be independent, or defined as a function of the moment. A proportionally variable axial load with a pre-defined proportionality factor with respect to moment is one of the loading cases with a dependent axial load. The input data at each step will be the “curvature and axial load” in a displacement-controlled analysis and the “moment and axial load” in a force-controlled analysis. In the iterative process to find the moment or curvature, the history of each element on the section is traced and updated at each step.

As example, for a displacement-controlled moment curvature analysis, for a step of given curvature and axial load, the location of the neutral axis is found through an iteration process to achieve the step axial load. The stress in each fiber element is calculated using its stress and strain in previous step, which are fixed during iteration, and are updated when the iteration converges to the step axial load with a desired accuracy.

For a force-deflection analysis, in addition to the section and material data, the length of the column and the model for the curvature distribution along the column, explained later, are defined. The monotonic or cyclic displacement at the tip of a column and the corresponding axial load serve as the input data for a displacement-controlled analysis. For a force-controlled analysis, the input data are the lateral force and the corresponding axial load. Axial load can be constant or variable. A variable axial load can change independently or can be defined as a function of lateral force. Based on the assumption on the curvature distribution, the moment-curvature at several analytically-selected sections along the column are monitored. Then, the lateral force for a given "displacement and axial load" in a displacement-controlled analysis, or the displacement for a given "lateral force and axial load" in a force-controlled case at the tip of the member is evaluated in an iteration process.

The accuracy of the results can be changed by refinement of the mesh, and the resolution of the output data can be increased by changing the number of data points within a specific range. This feature is especially useful when a certain limit, such as the first crack of a section, is of interest in the performance of a member.

2.2. Material models

Various material models can be used in analysis. They can be selected from the built-in list or user-defined as needed. In addition to commonly used material models, the following are developed specifically for the analytical program discussed in this paper.

2.2.1. Monotonic stress-strain model for steel

This flexible model, with 4 parameters can be tuned to simulate the behavior of different types of steel. The main intension was simulating the mild steel behavior based on the material test results conducted on samples of the steel. The parameters are as follows:

1. $\boldsymbol{K_1}$ is the ratio of the strain at start of the strain hardening to the yield strain.
2. $\boldsymbol{K_2}$ is the ratio of strain at peak stress to yield strain.
3. $\boldsymbol{K_3}$ is the ratio of ultimate strain to yield strain.
4. $\boldsymbol{K_4}$ is the ratio of the peak stress to yield stress.

The curve is assumed to be linear up to the yield point, and have a pure plastic deformation from the yield point up to a strain of $\boldsymbol{K_1}$ times the yield strain. The peak stress equal to $\boldsymbol{K_4}$ times the yield stress, is achieved at a strain of $\boldsymbol{K_2}$ times the yield strain. Rupture of steel occurs at a strain of $\boldsymbol{K_3}$ times the yield strain. A quadratic curve joins the point at the start of strain hardening, the peak stress and the rupture point. The mathematical formulation of this part of the model for $K_1\varepsilon_y \leq |\varepsilon| < K_3\varepsilon_y$ is as follows:

$$\sigma = \frac{E_s(1-K_4)[\varepsilon^2 + 2K_2(K_4-1)E_s|\varepsilon| + E_s\varepsilon_y(K_1^2K_4 - 2K_1K_2K_4 + K_2^2)]\varepsilon}{\varepsilon_y|\varepsilon|(K_1^2 - 2K_1K_2 + K_2^2)} \tag{1}$$

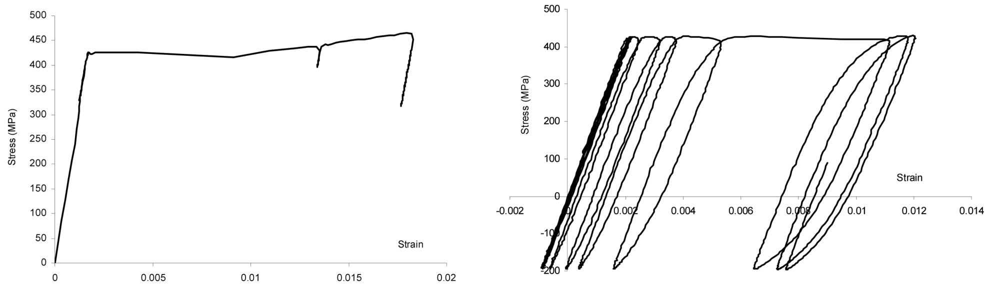

(a) (b)

Fig. 2 Material test results on steel monotonic (a) and Hysteresis (b) response

Where σ and ε are the steel stress and strain respectively, E_s is the steel modulus of elasticity, and ε_y is the yield strain of steel. This model and the associated Hysteresis rules were scaled against the material test data shown in Fig. 2.

2.2.2. Hysteresis stress-strain model for steel

The simple model developed and used for the hysteresis behavior of steel has the three major parts common in all hysteresis rules. Before any strain reversal, the stress and strain follow the monotonic stress-strain curve of steel as described earlier. At the turning point (strain reversal) the modulus of elasticity is assumed to be the same as initial modulus of elasticity of steel. The Bauschinger effect is considered in the model by changing the stiffness of steel to a portion of the initial stiffness beyond a certain stress in hysteresis response. For a more realistic implementation of strain hardening of steel, this ratio and the level at which the change occurs are different in the first and third quarters from their corresponding values in the second and fourth quarters of the coordinate plane.

Behavior of the model is symmetric with respect to the origin as a symmetrical monotonic stress-strain curve has been assumed for steel. Considering the limitations on the length of this paper, description of the behavior is provided in the flowchart shown in Fig. 3. Definitions of the symbols can be found beside the chart or in the list of notations. In the model, "Failure Flag, FF", is set to one when the element fails and the "Plastic Return Flag, PRF", is raised when a strain reversal occurs for a strain more than the steel yield strain.

2.2.3. Hysteresis stress-strain model for concrete

The monotonic stress-strain curve, selected from the built-in list or customized as shown in Fig. 4, serves as the envelope for the hysteresis stress-strain model of concrete developed and used in the analysis. At a strain reversal the hysteresis curve follows a parabolic path. The curve is concave-upward for a decreasing strain and has a slope of E_{c2} on the envelope curve. The stress decreases to zero when the tensile strength is ignored, or will decrease to the tensile strength, f_t with a slope of E_{ct} after the sign change of the stress. At a strain reversal with an increasing strain, the stress remains zero up to the latest strain corresponding to zero stress, ε_z, and then it grows on a concave-downward parabola which has a slope of E_{c1} on the strain axis. The stress increases up to the envelope curve and then follows that. It should be added that stiffness and strength degradation of concrete may be implemented in the model by linking the values of E_{c1}, E_{c2} and E_{ct} to the strain

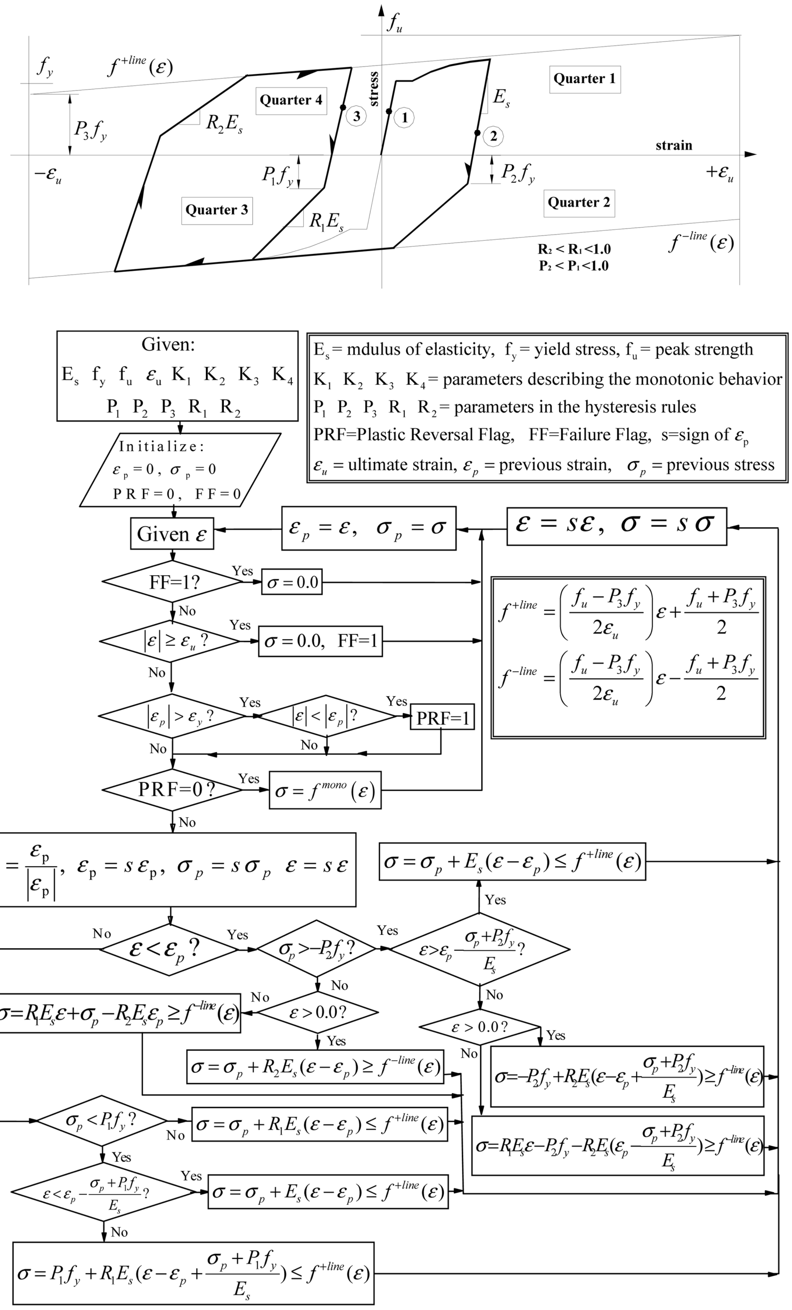

Fig. 3 Flowchart for the hysteresis rules of steel developed and used in the analysis

history. The mathematical description of the concrete hysteresis rules to find the stress σ for a new strain of ε, with a previous strain and stress of ε_p and σ_p respectively can be found in the flowchart shown in Fig. 5. Most of the symbols are defined in the chart or can be found in the list of notations.

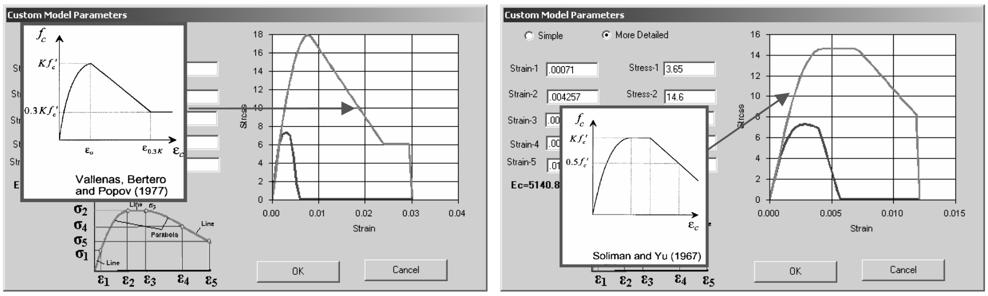

Fig. 4 Customized confined concrete model, to model any behavior

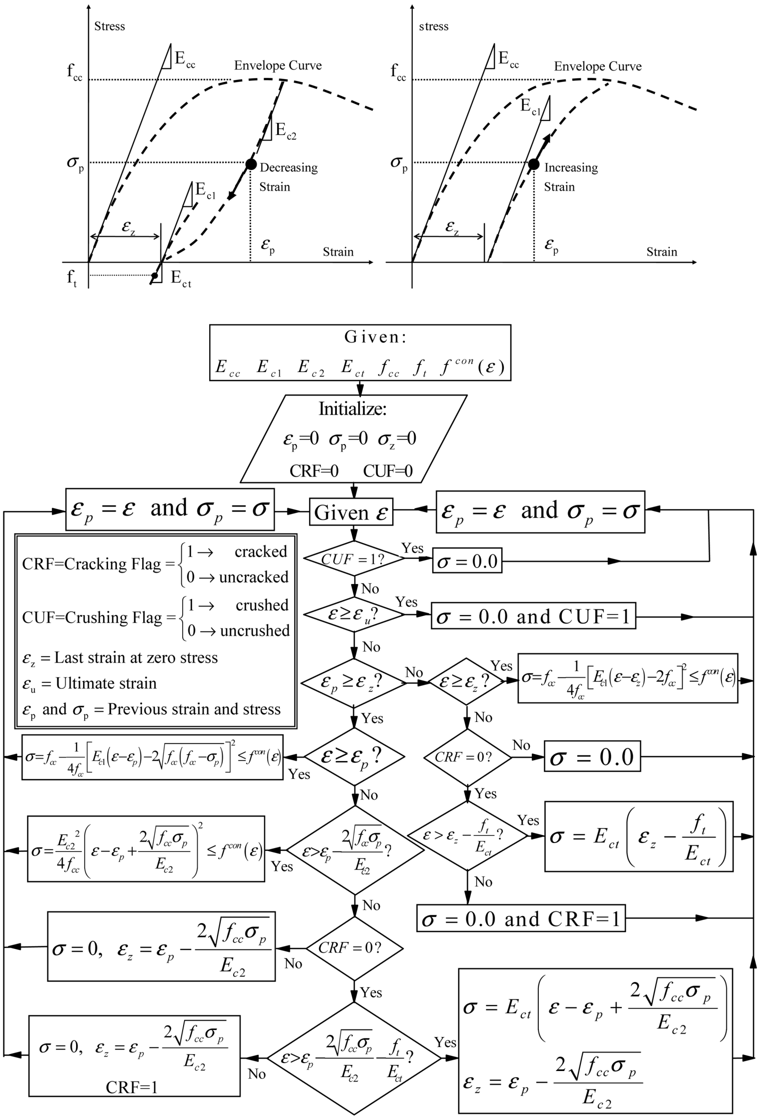

Fig. 5 Flowchart for the hysteresis rules of concrete developed and used in the analysis

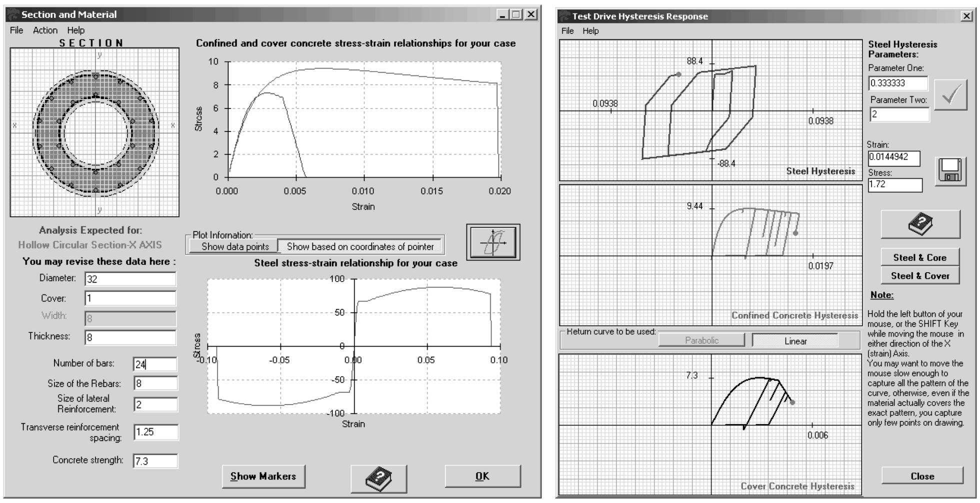

Fig. 6 View the monotonic and examine the hysteresis material models selected for a section

Each element on the section has 2 flags, CRF "Cracking Flag", and CUF "Crushing Flag", associated with the first tensile failure, and the first compression failure, respectively. Initially, an element is uncracked and uncrushed and $\varepsilon_z=\varepsilon_p=\sigma_p=0.0$. The deformation history of individual elements is tracked and updated at each step. An element will not have any tensile strength after the first crack and no compressive strength after the first crush in compression.

While E_{c1} and E_{c2} can be different in this model, these values have been chosen to be identical to E_{cc}, the initial stiffness of the concrete in the present version of the program. The computer application provides a friendly interface to view and examine the monotonic and especially hysteresis response of the material to be used in the analysis (Fig. 6). In a simplified version, the reversals can be linear with the same modulus of elasticity as the initial value of the stiffness.

2.3. Moment-curvature analysis

In general, for a fiber-based section analysis, concrete on the section of the model column is divided into elements in two directions to consider bi-axial independent moments and an arbitrary axial load, and steel bars are considered at their actual locations, as shown in Fig. 7. For a displacement controlled analysis, the neutral axis location is found for a given curvature and axial load level, with a predetermined accuracy, having the strain and stress history of each element on the section; and then, the corresponding moment is evaluated followed by updating the stress and strain state of each element. For a force controlled case, where at each step the moment and corresponding axial load are the input data, more computational effort is required for convergence of the iteration process to a desired level of accuracy. In any case, the hysteresis response of the section is evaluated by tracing the history of strain and stress of each single element on the section during analysis.

2.4. Force-deflection analysis

Deflection at the tip of the column is considered as a combination of the elastic deflection

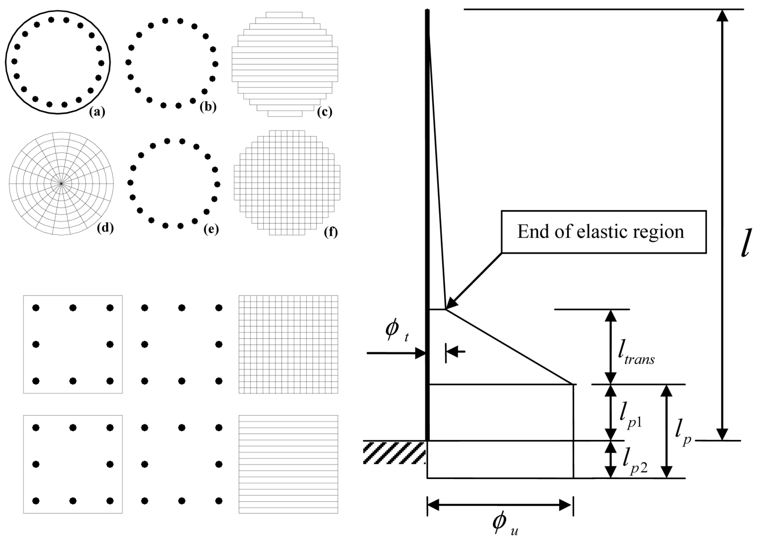

Fig. 7 Division of a section and assumption on curvature distribution along the member

associated with the elastic portion of the column, and plastic deflection associated with deformation within the plastic hinge region and also the rotation induced by the pull-out action of the rebar at the footing-column interface. Distribution of curvature within the plastic region is important especially for deflections beyond the maximum flexural strength of the member under a certain axial load. Most of the plastic hinge assumptions (Priestley and Park 1987) are developed considering monotonic deflections under a constant axial load. Experimental observations have revealed the effect of variation of axial load and cyclic deflections on the plastic hinge length. To address these effects, a method was developed considering various load and displacement patterns including a cyclic lateral displacement with a variable axial load. The assumption for the curvature distribution considers variation of the hinge length. Fig. 7 shows various regions of a column in terms of the curvature distribution. l_{p1}, with a uniform curvature of ϕ_u, is assumed to be equal to the depth of the section in the direction of analysis for members with a length to depth ratio of less than 12.5, and l_{p1}=0.08l for other cases, where l is the effective length of the member. l_{p2}= $0.15f_sd_b$ (or $0.022f_sd_b$ [SI]) where f_s is the maximum tensile stress on the section located at the column-footing interface and d_b is the diameter of the longitudinal bar with the maximum tensile stress. l_{p2}, with a uniform curvature of ϕ_u varies at each step based on the stress profile on the section. l_{trans} is not constant and increases as the location of the section experiencing the first yield moves upward. So, the portion of the member remaining within the elastic range is not constant and changes based on the loading and deflection condition. Portions of the member experiencing a deformation beyond the yield deformation in any step will fall out of this linear-elastic length for the rest of analysis. Initially the whole member is elastic. As the lateral displacement increases and depending on the axial load level, the section marked as the end of elastic region will move. The four regions on the member including the linear-elastic length, transition length, plastic length and the stress penetration or pull-out action length and their corresponding curvature distributions are updated at each step of analysis. Moment-curvature of two sections, one at the column-footing interface of a column, and the other at the end of the elastic region are monitored in this method. Note that for the latter, the location of the section changes based on the loading condition.

3. Verification of the program

To verify the functionality and performance of the application, results by others were reproduced by the program. Fig. 8 shows a comparison between the program predictions and analytical results by Bayrak and Sheikh (1997) and Sheikh and Uzumeri (1982) for the monotonic as well as cyclic moment curvature response of a rectangular section under a constant axial load using identical material models. Also, the section used in the example 2 of the Opensees online examples (OpenSees 2006) for moment-curvature analysis of a reinforced concrete section was analyzed by the application using identical geometry and reinforcement, and similar material properties, and the yield curvature was 0.005 m^{-1} (0.000127 in^{-1}) which compares very well with their estimation of 0.004999365 m^{-1} (0.000126984126984 in^{-1}) considering the specified accuracy for the application.

4. Performance prediction

The accuracy of the analytical predictions is partially dependent on the analytical models selected. Most of the recent models can provide a reasonable accuracy. Experimental data from six column specimens as shown in Fig. 9, tested under different loading conditions as detailed in Table 1, were

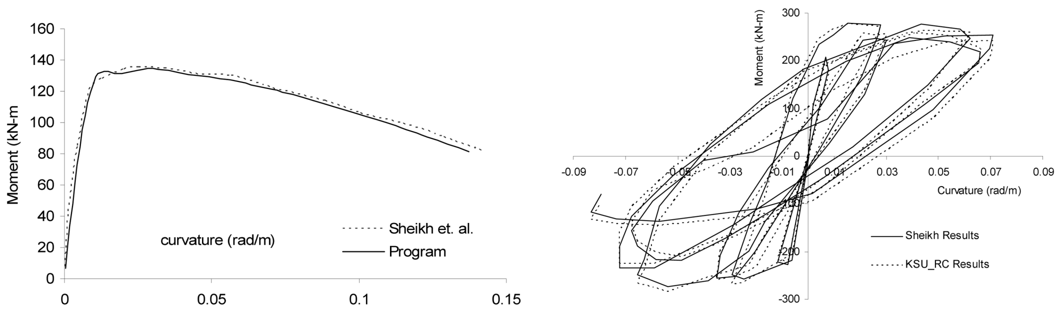

Fig. 8 Reproduction of the monotonic and cyclic moment-curvature response

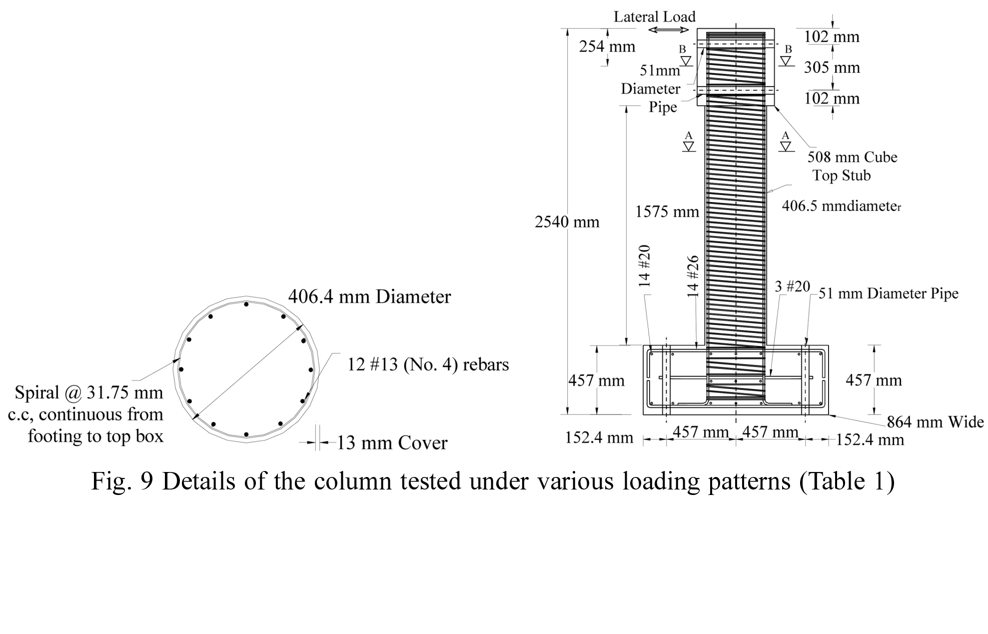

Fig. 9 Details of the column tested under various loading patterns (Table 1)

Table 1 Reinforcement and loading details of specimens

Case (Column)	Reinforcement (Nominal Properties)	Steel Ratio (Measured Properties)	Concrete Strength [MPa]	Lateral Force (Displacement)	Axial Load Case
No. 1	**Longitudinal** 12#13 **Transverse** W2.5 @ 32 mm (G 410) (ASTM G60) (E=199948 MPa) (f_y=413.7 MPa)	**Longitudinal** 1.17% (E=137895 MPa) (f_y=489.5 MPa) (f_u=579.2 MPa) **Transverse** 0.52% (E=164095 MPa) (f_y=468.8 MPa) (f_u=737.7 MPa)	49.3	Cyclic	Constant, 30% $A_g f'_c$
No. 2			49.3	Cyclic	Proportional, Lateral F/Axial p=1.2
No. 3			50.3	Monotonic	Constant, 30% $A_g f'_c$
No. 4			50.3	Monotonic	None
No. 5			50.3	Monotonic	Variable, Non-proportional
No. 6			50.3	Monotonic	Variable, Non-proportional

Note: 1 MPa is 0.145 ksi, No. 13 (SI) bar is equivalent to No. 4 (English)

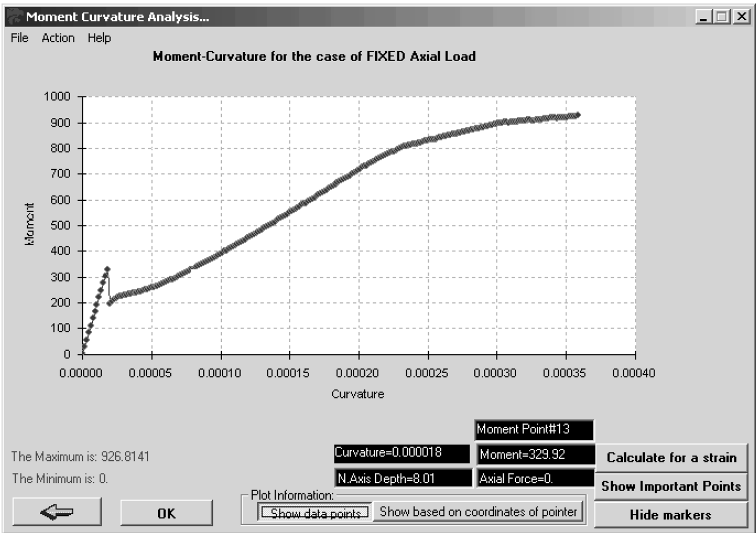

Fig. 10 The cracking of a section in a moment-curvature analysis, ignoring tension stiffening

used to validate performance prediction of the program using the default material models and hysteresis rules. The model columns had a circular section with a diameter of 406 mm, and a total height of 2,083 mm above the top of the footing. The effective length of the column was 1,829 mm, from the top of the footing to the application point of the lateral force. The longitudinal reinforcement consisted of 12 # 13 (nominal diameter = 12.5 mm) Grade 410 (ASTM G60) bars evenly distributed in a circle. One of the main goals of the program was prediction of the performance of a reinforced concrete member under a given loading pattern. This is especially important if some service limits are of special interest. Fig. 10 shows a window of the application showing the cracking of the section, in a moment curvature response analysis for demonstration. No tension stiffening is considered in analysis. A high value of the concrete tensile strength has intentionally been used for demonstration purpose. It is noteworthy that in a specific limit-state,

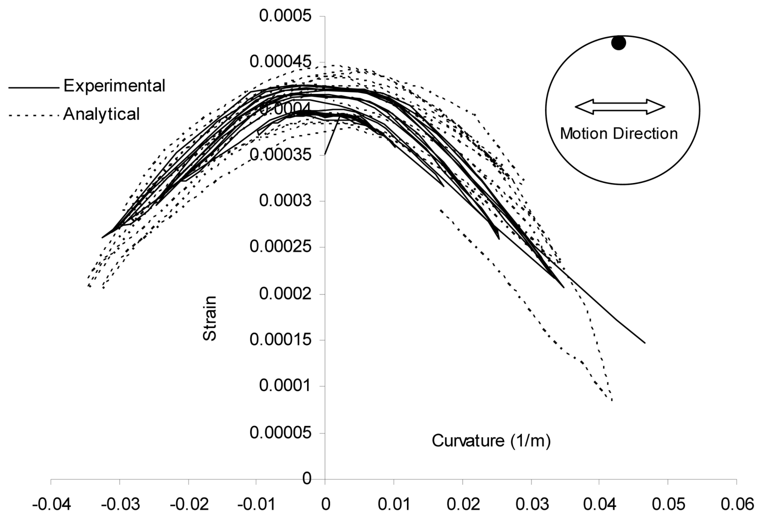

Fig. 11 Comparison of the experimental and calculated strain of a bar

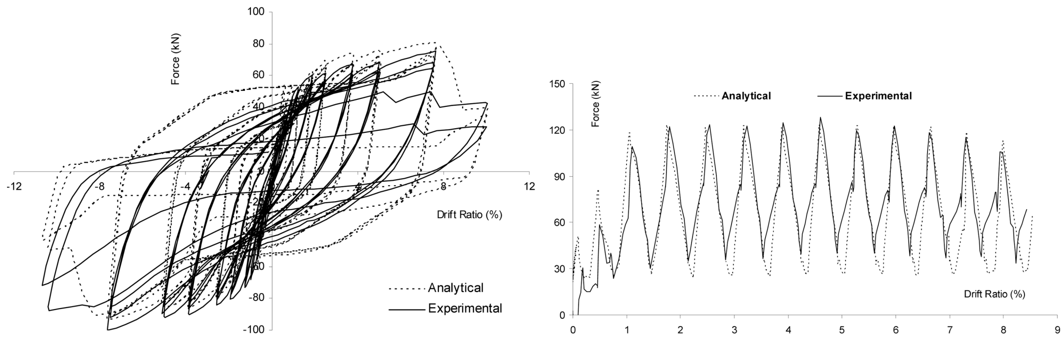

Fig. 12 Comparison of the experimental and calculated force-deflection for cases 2 and 5 (Table 1)

values of the existing state of strain, stress, deflection, etc., are evaluated and can be provided by the application. For example, the steel tensile and compressive strain, lateral deflection, depth of neutral axis, or other values of interest at the first crack, is readily available. Fig. 11 shows the analytical prediction for the strain of a bar at the center of a section close to the column-footing interface, compared to the recorded experimental strain. The test was conducted under a constant axial load of $0.3A_gf'_c$ and a cyclic lateral displacement.

Calculated performances of some of the cases mentioned in Table 1 are compared against test results in Figs. 12 and 13. Hysteresis rules and plastic hinge model developed by the author was selected for this analysis. These figs and other comparisons, not demonstrated here, show that the performance could be simulated with an acceptable accuracy for various loading patterns.

5. Parametric studies

As one of the goals, the program can also be used to examine various analytical models and

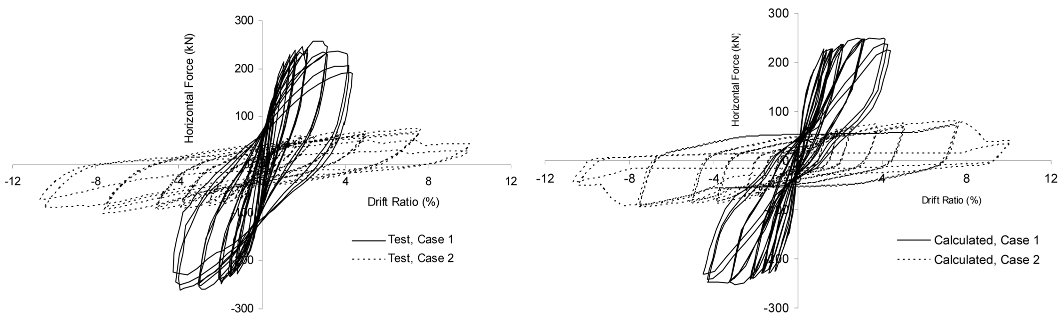

Fig. 13 Test results and calculated response for cases 1 and 2

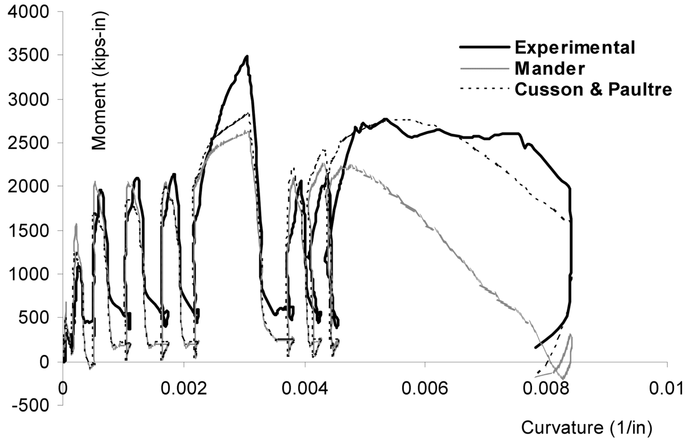

Fig. 14 Comparison of confined concrete models (for case 6)

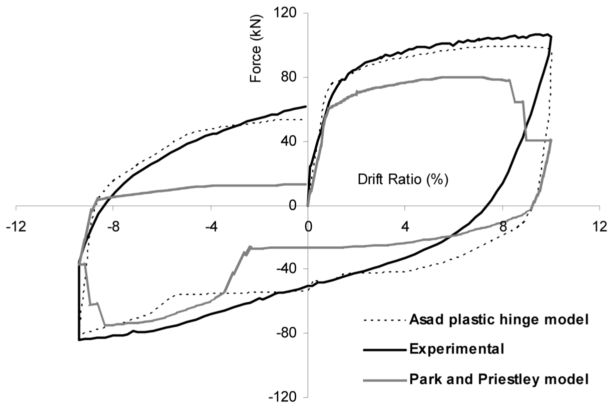

Fig. 15 Comparison of plastic hinge models (for case 4)

methods or refine a custom material model against test data. A parametric study can be conducted, comparing various models for confined concrete, keeping all other factors including geometry, reinforcement and other analytical methods and models fixed. Fig. 14 demonstrates a comparison between test results and the calculated moment-curvature response of the sixth case in Table 1 using two different models (Mander 1988, Cusson and Paultre 1995) for confined concrete stress-strain relationship. All other factors were the same for analysis. A detailed description of these comparisons can be found elsewhere (Esmaeily and Lucio 2006). Fig. 15, examines two models for “the curvature distribution on the column” in prediction of the force-deflection response of the fourth case in Table 1 compared to test data.

Parametric studies can also be conducted on axial as well as lateral loading pattern using the application and implementing proper material models as discussed earlier.

6. Conclusions

An analytical tool was developed using the commonly used analytical models and methods including analytical models and methods developed by the author to simulate the performance of reinforced concrete columns under various loading patterns. These models were implemented in a fiber-based moment-curvature and in turn force deflection analysis. The program was tested against analytical predictions by others for their available loading cases. It was also validated against the experimental results from six large-scale reinforced concrete columns tested under different loading scenarios, including non-sequential axial load variation and a cyclic lateral displacement.

While the program can be used for performance prediction of a reinforced concrete member under a specific loading pattern, it can also be used to evaluate various analytical models, such as confined concrete material models and plastic hinge methods.

The application can also be used to conduct a parametric study on the effects of the loading pattern on capacity-performance of a reinforced concrete member.

Analytical results, confirmed by the experimental data show that the axial force level and path play significant roles in the flexural strength and deformation capacity, and in general, the overall performance of a member.

This effect can be captured by a proper analysis process as described in this paper, and needs to be taken into consideration for assessment of the load carrying capacity and deformability of a reinforced concrete member. As example, the peak moments of a column under variable axial force may be less than the assumed or expected values using conventional design methods, assuming the same level of axial load.

It was observed that using a reasonable hysteresis material model for concrete, longitudinal steel and confining material, and a plastic hinge method as developed and used in this study along with conventionally used methods, as fiber model, can predict the performance with an acceptable accuracy. Predictions can be refined further by refinement of the models and considering tension stiffening and strength-stiffness degradation of the material.

References

Bayrak, O. and Sheikh, S. (1997), “High-strength concrete columns under simulated earthquake loading”, *American Concrete Inst. Struct. J.*, **94**(6), 708-722.

CSI Section Builder, Version 8.1.0, (2003), “Concrete, steel and composite sections”, Copyright 2002-2003, Computers and Structures, Inc. 1995 University Ave., Berkeley, CA 94704.

Cusson, D. and Paultre, P. (1995), “Stress-strain model for confined high-strength concrete”, *ASCE, J. Struct.*

Eng., **121**(3), 468-477.
Esmaeily, A. (2002), "KSU_RC, Moment-Curvature and Force-Deflection Analysis of a Reinforced Concrete Member", free window based educational computer application
Esmaeily, A. and Lucio, K. (2006), "Analytical performance of reinforced concrete columns using various confinement models", *ACI*, SP-238, 95-110.
Esmaeily, A. and Xiao, Y. (2004), "Behavior of reinforced concrete columns under variable axial loads", *ACI Struct, J.*, **101**(1), 124-132.
Esmaeily, A. and Xiao, Y. (2005), "Behavior of reinforced concrete columns under variable axial loads: analysis", *ACI Struct. J.,* **102**(5), 736-744.
Mander, J. B., Priestley, M. J. N. and Park R. (1988), "Theoretical stress strain model for confined concrete", ASCE *J. Struct. J.*, **114**(8), 1804-1825.
Mazzoni, S., McKenna, F., Scott, M. H. and Fenves, G. L. (2006), "Opensees for earthquake engineering simulation, user command, language manual, version 1.7.2", June, 2006, Pacific Earthquake Engineering Research Center, University of California, Berkeley, http://opensees.berkeley.edu/OpenSees/manuals/usermanual/index.html
OpenSees (2006), http://peer.berkeley.edu/~silvia/OpenSees/examplesprimer/html/
Prakash, V., Powell, G. and Campbell, S. (1993); DRAIN 2D User Guide V 1.10, University of California at Berkeley, CA.
Priestley, M. J. N. and Park, R. (1987), "Strength and ductility of concrete bridge columns under seismic loading", *ACI Structural J.*, Title No. 84-S08, 61-75.
Sheikh, S. A. and Uzumeri, S. M. (1982), "Analytical model for concrete confinement in tied columns", *J. Struct. Eng., ASCE,* **108**, No. ST12, 2703-2722.

Notation

α = parameter used in the hysteresis stress-strain model of steel
ε = measured strain by the strain gage and also steel strain
ε_c = concrete strain
ε_{cc} = confined concrete strain at the maximum strength (f'_{cc})
ε_p = strain of steel at previous point in a hysteresis model
ε_u = ultimate strain of steel
ε_y = yield strain of steel
ε_z = latest strain corresponding to zero stress in concrete hysteresis rules
σ = steel stress
σ_p = stress of steel at previous point in a hysteresis model
CRF = cracking flag in concrete Hysteresis rules
CUF = crushing flag in concrete Hysteresis rules
E = modulus of elasticity
E_{c1} = initial modulus of elasticity of concrete
E_{c2} = secondary modulus of elasticity of concrete
E_{ct} = modulus of elasticity of concrete on tensile side
E_s = steel modulus of elasticity
FF = failure flag
K_1 to K_4 = Parameters for monotonic stress-strain relationship of steel
P_1 , P_2 = Parameters for hysteresis stress-strain model of steel
c = cover concrete thickness
f_y = yield stress of steel

f_c	=	concrete stress
f'_c	=	concrete compressive strength
f'_{cc}	=	confined concrete maximum strength
f_u	=	steel stress at ultimate strain of steel (ε_u)
f_t	=	tensile strength of plain concrete
x	=	ratio of strain (ε_c) to the strain at peak stress (ε_{cc})

CM